

RESEARCH  
PAPER



# Global patterns in the vulnerability of ecosystems to vegetation shifts due to climate change

Patrick Gonzalez<sup>1\*</sup>, Ronald P. Neilson<sup>2</sup>, James M. Lenihan<sup>2</sup> and Raymond J. Drapek<sup>2</sup>

<sup>1</sup>Center for Forestry, University of California, Berkeley, CA 94720-3114, USA, <sup>2</sup>Pacific Northwest Research Station, USDA Forest Service, Corvallis, OR 97331, USA

## ABSTRACT

**Aim** Climate change threatens to shift vegetation, disrupting ecosystems and damaging human well-being. Field observations in boreal, temperate and tropical ecosystems have detected biome changes in the 20th century, yet a lack of spatial data on vulnerability hinders organizations that manage natural resources from identifying priority areas for adaptation measures. We explore potential methods to identify areas vulnerable to vegetation shifts and potential refugia.

**Location** Global vegetation biomes.

**Methods** We examined nine combinations of three sets of potential indicators of the vulnerability of ecosystems to biome change: (1) observed changes of 20th-century climate, (2) projected 21st-century vegetation changes using the MC1 dynamic global vegetation model under three Intergovernmental Panel on Climate Change (IPCC) emissions scenarios, and (3) overlap of results from (1) and (2). Estimating probability density functions for climate observations and confidence levels for vegetation projections, we classified areas into vulnerability classes based on IPCC treatment of uncertainty.

**Results** One-tenth to one-half of global land may be highly (confidence 0.80–0.95) to very highly (confidence  $\geq 0.95$ ) vulnerable. Temperate mixed forest, boreal conifer and tundra and alpine biomes show the highest vulnerability, often due to potential changes in wildfire. Tropical evergreen broadleaf forest and desert biomes show the lowest vulnerability.

**Main conclusions** Spatial analyses of observed climate and projected vegetation indicate widespread vulnerability of ecosystems to biome change. A mismatch between vulnerability patterns and the geographic priorities of natural resource organizations suggests the need to adapt management plans. Approximately a billion people live in the areas classified as vulnerable.

## Keywords

**Adaptation, biome change, climate change, dynamic global vegetation model, natural resource management, vegetation shifts, vulnerability.**

\*Correspondence: Patrick Gonzalez, Center for Forestry, 163 Mulford Hall, University of California, Berkeley, CA 94720-3114, USA.  
E-mail: pgonzalez@cal.berkeley.edu

## INTRODUCTION

Climate change is shifting vegetation latitudinally and elevationally at sites in boreal, temperate and tropical ecosystems (IPCC, 2007a,b; Rosenzweig *et al.* 2008). Changes in climate alter plant mortality and recruitment by exceeding physiological thresholds and changing wildfire and other disturbances. The resulting replacement of dominant plant species can entirely change the biome of an area and shift the global

location of biomes. Such fundamental changes can alter ecosystem structure and the provision of ecosystem services to people. A lack of spatial data on vulnerability has, in part, hindered organizations that manage natural resources from identifying priority areas for adaptation measures (Hannah *et al.*, 2002; Brooks *et al.*, 2006). Analyses of novel future climates (Williams *et al.*, 2007) and simulations using dynamic global vegetation models (DGVMs; Scholze *et al.*, 2006; Alo & Wang, 2008; Sitch *et al.*, 2008; Jones *et al.*, 2009) have projected

future shifts in climate and vegetation due to climate change.

Here, we explore the application of spatial analyses of climate observations and DGVM projections to the identification of areas vulnerable to vegetation shifts and potential refugia. We examine three sets of potential indicators of the vulnerability of ecosystems to biome change: (1) observed changes of 20th-century climate, (2) projected 21st-century vegetation changes using a DGVM under three IPCC emissions scenarios, and (3) overlap of results from (1) and (2). We use IPCC uncertainty criteria to develop a vulnerability classification framework that natural resource managers could use to identify priority areas for adaptation measures.

Climatic and ecological evidence supports the use of observed climate change as a potential indicator of vulnerability of ecosystems to biome change:

1. Climate exerts dominant control on the global distribution of biomes, a fundamental basis of plant biogeography (Woodward *et al.*, 2004). Changes in temperature and precipitation shifted global biomes latitudinally across continents in the late Quaternary (Jackson & Overpeck, 2000; Davis & Shaw, 2001), demonstrating the fundamental influence of climate on biomes.
2. Comprehensive meta-analyses (Parmesan & Yohe, 2003; Rosenzweig *et al.*, 2007, 2008) of published ecological research demonstrate that climate change in the 20th century has shifted plant ranges (37 species) and phenology (1161 species) in ecosystems around the world. More than 90% of time series of ecological data exhibited changes in the direction expected with warming temperatures. Many of the range shifts also changed the biomes of the ecosystems studied. The meta-analyses examined all time series, including those showing no change or change opposite to the direction expected with warming, and accounted for publication bias that might favour positive results.
3. We conducted a comprehensive search of the published literature (see Appendix S1 in Supporting Information) for cases of field research that examined long-term trends of biomes in areas where climate (not land-use change or other factors) predominantly influenced vegetation and found 15 cases documenting biome shifts in boreal, temperate and tropical ecosystems in the 20th century and four cases that found no biome shift (Appendix S1). The number of biome changes observed in the field and attributed to climate change indicates that 20th-century changes in temperature and precipitation are altering many ecosystems. Among the cases of observed biome change, observed temperature or precipitation shifted as much as one-half to two standard deviations from 20th-century mean values (Gonzalez, 2001; Peñuelas & Boada, 2003; Beckage *et al.*, 2008; Kullman & Öberg, 2009).
4. Because vegetation often responds slowly to changes in environmental conditions, a time lag between a change in climate and a shift in vegetation can commit an ecosystem to biome change long before any response manifests itself (Rosenzweig *et al.*, 2007; Jones *et al.*, 2009). Slow rates of seed dispersal and tree growth and long periods for physiological changes in plants contribute to time lags. Therefore, future vulnerability is partially a function of past climate change.

Observed changes in temperature and precipitation provide indicators of the potential change of the biome of an ecosystem. Using observed climate data accounts for the impact of climate change that has already occurred. This can provide a more complete assessment of vulnerability than future projections alone. We look at the three methods – observations alone, projections alone and the overlap of observations and projections – in parallel, not as mutually exclusive replacements for each other, to reveal areas where the ensemble of methods consistently identifies vulnerable areas or potential refugia.

## METHODS

### Definitions and general approach

In quantifying potential indicators of vulnerability, we followed IPCC definitions of likelihood, confidence and vulnerability. Likelihood is the probability of an outcome having occurred or occurring in the future (Schneider *et al.*, 2007). We estimated likelihoods of observed changes of 20th-century climate from probability density functions of 102 years of observation data. Confidence is the subjective assessment that any statement about an outcome will prove correct (Schneider *et al.*, 2007). We estimated confidence levels of DGVM projections from the output of a set of different general circulation models (GCMs).

Vulnerability to climate change is the degree to which a system is susceptible to, and unable to cope with, adverse effects (IPCC, 2007b). Here, vulnerability is the susceptibility of an ecosystem to a change in its biome, where biomes are major vegetation types that are characterized by the same life-form (Woodward *et al.*, 2004). Vulnerability is a function of three components: exposure, sensitivity and adaptive capacity. In our analysis, observed and projected climate changes indicated degree of exposure. Deviation of climate from long-term mean values (in the absence of complete spatial data on early 20th-century global vegetation) and modelled changes of future vegetation provide indicators of ecosystem response, which combines sensitivity and adaptive capacity. An ecosystem with low sensitivity and/or high adaptive capacity would respond with modest changes, indicating lower vulnerability.

In the IPCC (2007a) treatment of uncertainty, confidence spans five levels: very high (at least a 9 out of 10 chance of an outcome proving correct), high (about an 8 out of 10 chance), medium (about a 5 out of 10 chance), low (about a 2 out of 10 chance) and very low (less than 1 out of 10 chance). We used these levels to divide results into vulnerability classes.

### Equal-area projection of spatial data

All original sets of global climate, vegetation, fire and population data were unprojected rasters in the geographic reference system, where the surface area of pixels varied with latitude. To accurately calculate land areas, we divided all global files into six continental files and projected each continent to Lambert azimuthal equal-area projection at a spatial resolution of 50 km, using the parameters of the International Geosphere–Biosphere

Programme Global Land Cover Characteristics database (<http://edc2.usgs.gov/gllcc>). The data cover the terrestrial area of the world, except Antarctica.

### Observed climate and fire

We calculated observed climate trends in the University of East Anglia Climate Research Unit TS 2.1 data set (Mitchell & Jones, 2005) by linear least squares regression of mean annual temperature and annual precipitation versus time for the period 1901–2002. For the correlation coefficients, we also calculated the statistical significance ( $P_r$ ).

Although the biological importance of a change in climate will tend to increase as  $P_r$  increases,  $P_r$  does not give a direct measure of the magnitude of the change. In contrast, the histogram of 102 annual temperature or precipitation values forms a probability density function and deviation of the value of the change in temperature or precipitation in a century (given by the slope of the regression) from the 102-year mean indicates the statistical significance of the rate of change.

For each of 58,267 land pixels, we calculated

$$C_{\text{temperature}} = m_{\text{temperature}} \left( \frac{100 \text{ years}}{\text{century}} \right) \quad (1)$$

where  $C_{\text{temperature}}$  is the rate of observed temperature change ( $^{\circ}\text{C century}^{-1}$ ) and  $m_{\text{temperature}}$  is the slope of the regression ( $^{\circ}\text{C year}^{-1}$ ) and

$$C_{\text{precipitation}} = \left( \frac{m_{\text{precipitation}}}{\mu_{\text{precipitation}}} \right) \left( \frac{100 \text{ years}}{\text{century}} \right) \quad (2)$$

where  $C_{\text{precipitation}}$  is the fractional rate of observed precipitation change ( $\text{century}^{-1}$ ),  $m_{\text{precipitation}}$  is the slope of the regression ( $\text{mm year}^{-2}$ ), and  $\mu_{\text{precipitation}}$  is mean 1901–2002 precipitation ( $\text{mm year}^{-1}$ ).

We calculated the probabilities of the observed climate changes:

$$P_{\text{climate}} = \text{erf} \left( \frac{C_{\text{climate}}}{\sigma_{\text{climate}} (1 \text{ century}) \sqrt{2}} \right) \quad (3)$$

where the subscript 'climate' denotes temperature or precipitation,  $P_{\text{climate}}$  is the probability that  $C_{\text{temperature}}$  or  $C_{\text{precipitation}}$  falls within a calculated number of standard deviations of the mean,  $\text{erf}(x)$  is the error function, and  $\sigma$  is the 1901–2002 standard deviation, such that  $P_{\text{climate}} = 0.68$  at  $1\sigma$ ,  $0.95$  at  $2\sigma$  and  $0.99$  at  $3\sigma$ .

We classified pixels into five vulnerability classes (IPCC, 2007a): very high ( $P_{\text{climate}} \geq 0.95$ ), high ( $0.95 > P_{\text{climate}} \geq 0.8$ ), medium ( $0.8 > P_{\text{climate}} \geq 0.2$ ), low ( $0.2 > P_{\text{climate}} \geq 0.05$ ) and very low ( $P_{\text{climate}} < 0.05$ ). We used the value of  $P$  that was greater between temperature and precipitation because a significant change in either parameter could cause a change in biome (Woodward *et al.*, 2004). Although the absolute magnitude of or variation in  $C_{\text{temperature}}$  or  $C_{\text{precipitation}}$  that may cause a biome change will differ by ecosystem, the likelihood of change will

increase with the deviation of climate from the conditions under which the vegetation of a location developed.

To explore potential impacts of fire, we also calculated trends in the global fire database of Mouillot & Field (2005) by linear least squares regression of fire frequency for the period 1900–2000 versus time.

### Projected climate

We used an ensemble of three GCMs to represent lower (CSIRO Mk3; Gordon *et al.* 2002), medium (HadCM3; Johns *et al.*, 2003) and higher (MIROC 3.2 medres; Hasumi & Emori, 2004) temperature sensitivity for the period 2000–2100. GCM runs for the three emissions scenarios used in the IPCC Fourth Assessment Report (AR4; IPCC, 2007a,b) represent lower (B1), medium (A1B) and higher (A2) greenhouse gas emissions. The nine GCM–emission scenario combinations bracket a substantial part of the range of temperature projections of the 59 AR4 combinations. Constraints of funding and the unavailability of vapour pressure output (required for the MC1 DGVM) from some GCMs prevented analysis of all 59 combinations, necessitating the use of a bracketing approach.

GCM output came from the World Climate Research Programme Coupled Model Intercomparison Project Phase 3 multi-model dataset (<https://esg.llnl.gov:8443/index.jsp>). We statistically downscaled GCM output from  $2.5^{\circ}$  latitude by  $3.75^{\circ}$  longitude spatial resolution to  $0.5^{\circ}$  spatial resolution in three steps: (1) calculation of the difference (temperature) or ratio (precipitation, vapour pressure) of a GCM-projected future value with the GCM-modelled 1961–90 mean, (2) bilinear interpolation of the differences or ratios at a spatial resolution of  $0.5^{\circ}$  with a  $2 \times 2$  kernel, and (3) addition of the temperature difference to or multiplication of the precipitation and vapour pressure ratios by the  $0.5^{\circ}$  spatial resolution 1961–90 observed mean values (Mitchell & Jones, 2005).

### Projected vegetation and fire

To model potential vegetation and wildfire, we ran the MC1 dynamic global vegetation model (Daly *et al.*, 2000; Lenihan *et al.*, 2008) on the nine GCM–emissions scenario combinations. MC1 uses five climate variables (monthly mean, maximum and minimum temperature; precipitation; vapour pressure) and five soil variables (soil depth; bulk density; clay, sand and rock fractions) to run interacting modules of biogeography, biogeochemistry and wildfire. The climate variables required by MC1 limited the GCMs that we could use to those with available output. The biogeography module identifies the potential vegetation type of a pixel by modelling plant life-form as distinguished by leaf characteristics. The relative proportion of different woody life-forms is determined at each annual time step by position along gradients of minimum temperature and growing season precipitation. The minimum temperature gradient runs from evergreen needleleaf dominance ( $-15^{\circ}\text{C}$ ) through deciduous broadleaf dominance to broadleaf evergreen dominance ( $18^{\circ}\text{C}$ ). The relative proportion of C3 and C4

grasses is determined by estimating potential productivity as a function of soil temperature during the three warmest consecutive months. The biogeochemistry module calculates the biomass of trees and grasses for each pixel by modelling net primary productivity (NPP), organic matter decomposition and carbon, nitrogen and water cycling. MC1 simulates changes to plant physiology, nutrient cycling, water use and biomass due to changes in atmospheric CO<sub>2</sub>. We modelled NPP trends using the 23% increase to a doubling of pre-industrial atmospheric CO<sub>2</sub> (logarithmic biotic growth factor  $\beta = 0.60$ ) observed at a broad range of sites (Norby *et al.*, 2005). The wildfire module simulates wildfire occurrence and behaviour based on fuel loadings and fuel and soil moisture and calculates resulting changes in plant life-form mixtures and biomass. We modelled potential fire with no human suppression. The modelled plant life-form mixture from the biogeography module together with woody plant and grass biomass from the biogeochemistry module determine the vegetation type that occurs at each pixel each year. We combined the 34 MC1 potential vegetation types (Kuchler, 1964; VEMAP Members, 1995) into 13 biomes (FAO, 2001; Woodward *et al.*, 2004) and used the biome that MC1 modelled for each pixel for the majority of years during each of two periods (1961–90, 2071–2100) to represent the average vegetation for each period.

To assess the accuracy of MC1, we validated MC1 output against observed global vegetation and fire data. We compared the areas of forest and non-forest modelled by MC1 for 1961–90 climate with areas of forest and non-forest in remote sensing-derived Global Land Cover 2000 data (Bartholomé & Belward, 2005), excluding agricultural and urban areas. We also compared areas of fire rotation period  $\leq 35$  years for 1951–2000 modelled by MC1 and derived from field observations and remote sensing (Mouillot & Field, 2005). We calculated areas of agreement and the kappa statistic (Cohen, 1960; Monserud & Leemans, 1992).

For each of 54,433 land pixels, we estimated the level of confidence in projections that the biome of an area may change ( $c_{\text{projection}}$ ) as the fraction of the nine GCM–emission scenario combinations that project the same type of biome change for a pixel. The converse of the confidence in projections of biome change ( $1 - c_{\text{projection}}$ ) is the confidence in a projection of no biome change. We classified pixels into five classes of vulnerability (IPCC, 2007a): very high ( $c_{\text{projection}} \geq 0.95$ ), high ( $0.95 > c_{\text{projection}} \geq 0.8$ ), medium ( $0.8 > c_{\text{projection}} \geq 0.2$ ), low ( $0.2 > c_{\text{projection}} \geq 0.05$ ) and very low ( $c_{\text{projection}} < 0.05$ ). We also estimated the level of confidence and vulnerability classes for each emissions scenario.

### Overlap of observed and projected vulnerability

For all nine GCM–emission scenario combinations and for each emissions scenario, we determined the overlap of the vulnerability classes that were separately derived from observed climate and projected vegetation by classifying pixels where both  $P_{\text{climate}}$  and  $c_{\text{projection}}$  fell within the same range into five vulnerability classes. To avoid under- or overestimation of the vulnerability of certain areas of very high or very low  $P_{\text{climate}}$  or  $c_{\text{projection}}$ , we

included two exceptional combinations of medium vulnerability (very high  $P_{\text{climate}}$  and medium  $c_{\text{projection}}$ , very high  $c_{\text{projection}}$  and medium  $P_{\text{climate}}$ ) in the high class and two (very low  $P_{\text{climate}}$  and medium  $c_{\text{projection}}$ , very low  $c_{\text{projection}}$  and medium  $P_{\text{climate}}$ ) in the low class (Appendix S2).

### Population

To estimate the human population living in each vulnerability class, we used AD 2000 population from the Center for International Earth Science Information Network Gridded Population of the World dataset, Version 3 (<http://sedac.ciesin.columbia.edu/gpw>). We masked the population data by the area of each vulnerability class to calculate the total number of people living in each area.

### Limitations of the methods

For the analyses of observed climate data, equation 3 assumes a roughly normal distribution of annual climate values. The use of mean annual temperature and total annual precipitation is a simplification that assumes approximate correlation to minimum temperature and other climate parameters that affect the distribution of biomes. It also assumes that average climate conditions over long periods more strongly affect biomes than short-term climate extremes and variability, which can be important for individual species. Although the values of  $P_{\text{climate}}$  are not calibrated to precise magnitudes and timings of biome change, which may differ by vegetation type, observed temperature or precipitation shifts of one-half to two standard deviations from 20th-century mean values over the course of 50–100 years have caused changes in a diverse set of biomes (Gonzalez, 2001; Peñuelas & Boada, 2003; Beckage *et al.*, 2008; Kullman & Öberg, 2009).

For future emissions scenarios, IPCC has not estimated probabilities of occurrence, so we assumed equal probabilities of the three scenarios that IPCC selected for AR4 (IPCC, 2007a,b). The scenarios do not include the hottest defined scenario, A1FI. If actual global emissions exceed emissions under A1FI (Raupach *et al.*, 2007), then our analysis may provide a lower estimate of vulnerability than might occur if the world continues unmitigated emissions of greenhouse gases, although it would be possible to use the A2 results. Precipitation patterns vary across the three GCMs more than temperature patterns.

For future projections, the analysis assumes reasonable accuracy of GCMs and MC1. IPCC (2007a) has validated GCM skill. We validated MC1 output against observed global vegetation (Bartholomé & Belward, 2005) and fire (Mouillot & Field, 2005). Data from only one DGVM were available for this research, but future analyses would benefit from output from several DGVMs. The analysis compares conditions under standard 30-year climatology periods, but does not examine the timing or seasonality of changes.

For the overlap of observed and projected vulnerability classes, equal weighting of past observations and future projections is a normative decision, though it reflects the importance

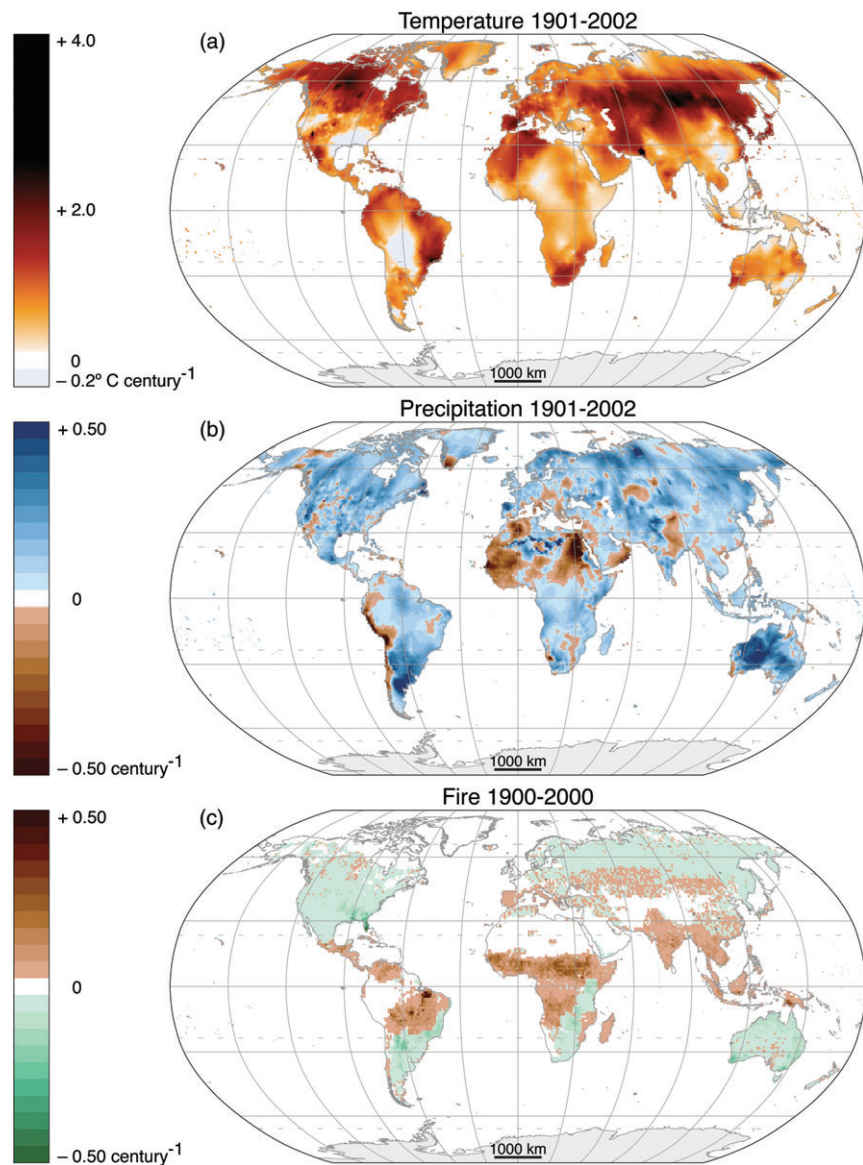


**Figure 1** Observed climate and fire trends. Rates of change derive from linear least squares regression of (a) temperature 1901–2002 (Mitchell & Jones, 2005), (b) precipitation 1901–2002 (Mitchell & Jones, 2005), and (c) fire frequency 1900–2000 (Mouillot & Field, 2005) versus time. The figure shows precipitation and fire trends as fractional change per century. (All global maps are in the Robinson projection.)

of both realized and potential impacts of climate change and the use of one century of data from the past and one century of data for the future.

## RESULTS

### Observed changes in climate and fire

Temperature increased on 96% of global land (Fig. 1a) in the 20th century with significant ( $P_i \leq 0.05$ ) increases on 76% of global land. Average temperature increased on every continent (Table 1). The greatest warming has occurred in boreal regions. Precipitation increased on 80% of global land in the 20th century (Fig. 1b, Table 1), with significant increases on 28% of global land and significant decreases on 2%. Global average precipitation increased at a fractional rate ( $\pm$  SD) of  $0.08 \pm 0.14$  century<sup>-1</sup>. The West African Sahel, the upper Nile region, and coastal Peru have experienced the greatest decreases in precipitation.

Fire frequency in the 20th century decreased on two-fifths of global land, slightly greater than the area of increase (Fig. 1c, Table 1). Global average fire frequency ( $\pm$  SD) was  $0.04 \pm 0.06$  year<sup>-1</sup>, corresponding to a rotation period ( $\pm$  SD) of  $27 \pm 17$  years. Global average fire frequency increased at a fractional rate ( $\pm$  SD) of  $0.004 \pm 0.04$  century<sup>-1</sup>. Decreased fire across Australia, North America and Russia reveals extensive suppression, while increased fire across the tropics shows increased burning to clear agricultural fields (Mouillot & Field, 2005). Due to these human influences, we used observed temperature and precipitation, but not fire, as potential indicators of vulnerability.

### Projected changes in climate

GCMs project widespread temperature increases and precipitation changes by 2100 (Fig. 2a,b, Table 1), including global average temperature increases of  $2.4\text{--}4$  °C century<sup>-1</sup> and global

**Table 1** Observed and projected rates of temperature change ( $\pm$  standard deviation) and fractions of continental or global land areas subject to precipitation and wildfire changes.

Continent	20th-century observations					21st-century projections				
	Temperature increase ( $^{\circ}\text{C century}^{-1}$ )	Precipitation increase (fraction (%) of continental or global area)	Precipitation decrease (fraction (%) of continental or global area)	Fire increase	Fire decrease	Temperature increase ( $^{\circ}\text{C century}^{-1}$ )	Precipitation increase (fraction (%) of continental or global area)	Precipitation decrease (fraction (%) of continental or global area)	Wildfire increase	Wildfire decrease
Africa	$0.55 \pm 0.36$	59	41	49	18	$3.5 \pm 0.5$	49	48	33	14
Asia	$0.94 \pm 0.54$	84	16	34	40	$2.1 \pm 0.3$	48	48	34	13
Australia	$0.41 \pm 0.31$	91	9	25	68	$2.6 \pm 0.5$	77	23	39	24
Europe	$0.85 \pm 0.33$	83	17	28	52	$1.8 \pm 0.3$	78	22	38	24
North America	$0.83 \pm 0.50$	90	10	9	56	$2.9 \pm 0.4$	79	21	37	25
South America	$0.62 \pm 0.49$	82	18	43	28	$2.4 \pm 0.3$	49	50	41	9
World	$0.74 \pm 0.45$	80	20	33	40	$2.8 \pm 0.8$	50	68	37	14
						$4.6 \pm 1.2$	32	33	32	17
						$4.0 \pm 1.2$	67	30	30	28
						$2.8 \pm 0.8$	70	26	28	28
						$4.4 \pm 0.8$	73	30	24	23
						$3.9 \pm 0.7$	70	26	23	24
						$2.7 \pm 0.5$	74	27	24	23
						$3.7 \pm 0.9$	73	71	29	11
						$3.2 \pm 0.7$	28	30	29	11
						$2.2 \pm 0.5$	30	63	28	11
						$4.0 \pm 0.8$	36	39	33	19
						$3.4 \pm 0.7$	60	38	32	19
						$2.4 \pm 0.5$	61	38	32	20
							61	38	32	20

We calculated observed climate changes from 1901–2002 CRU TS 2.1 data (Mitchell & Jones, 2005) and observed fire changes from 1900–2000 data (Mouillot & Field, 2005). Projected climate changes for 1990–2100 come from IPCC (2007a) data for emissions scenarios A2 (top), A1B (middle) and B1 (bottom). Projected wildfire changes for 2000–2100 come from MC1 results.

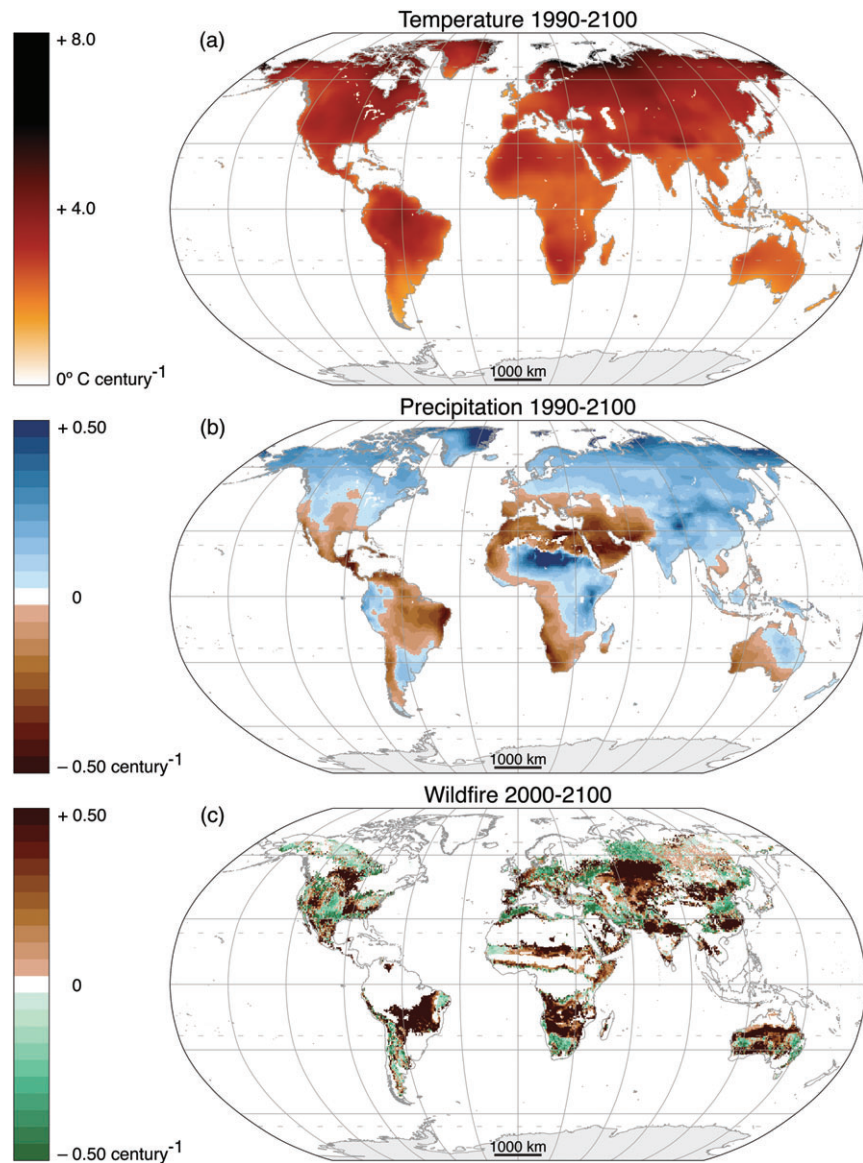


**Figure 2** Projected climate and fire trends. Rates of change are shown for the three general circulation model ensemble for IPCC (2007a) emissions scenario A1B for (a) temperature between the periods 1961–90 and 2071–2100, (b) precipitation for the same periods, and (c) wildfire frequency between the periods 1951–2000 and 2051–2100. Spatial patterns for IPCC emissions scenarios B1 and A2 are similar to patterns for A1B, but differ in magnitude.

average precipitation increases at fractional rates of 0.03–0.04 century<sup>-1</sup>. MC1 projects that a third of global land may experience an increase in wildfire frequency (Fig. 2c, Table 1), with global average increases at fractional rates of 0.21–0.29 century<sup>-1</sup>.

### Projected vegetation shifts

MC1-modelled 1961–90 vegetation (Fig. 3a) generally follows observed patterns of global biomes (FAO, 2001; Bartholomé & Belward, 2005), with modelled forest and non-forest areas corresponding broadly (agreement 77%, kappa = 0.53) to remote sensing-derived land cover (Bartholomé & Belward, 2005), excluding agricultural and urban areas. This kappa value is in the range considered ‘fair’ (Monserud & Leemans, 1992). MC1-modelled areas of wildfire rotation period  $\leq 35$  years for 1951–2000 correspond less closely (agreement 66%, kappa = 0.34) to wildfire observations (Mouillot & Field, 2005).

MC1 projects potentially extensive biome changes under the 2071–2100 scenarios (Fig. 3b). Areas where all combinations project the same biome change ( $c_{proj} \sim 1$ ) cover 8% of global land (Fig. 3c). Temperate mixed forest shows the highest fractional areas of projected change, while desert shows the lowest (Appendix S3). Projected changes in wildfire frequency (Fig. 2c) drive many of the projected biome changes. Differences among GCMs caused more variation in biome projections than differences among emissions scenarios. The B1, A1B and A2 ensembles disagree on 25, 32 and 30% of global land, respectively, while the CSIRO, HadCM3 and MIROC emissions scenario sets for each GCM disagree on 17, 17 and 18% of global land, respectively.

### Vulnerability

Observed climate and vegetation projections indicate that one-tenth to one-half of global land may be highly to very highly

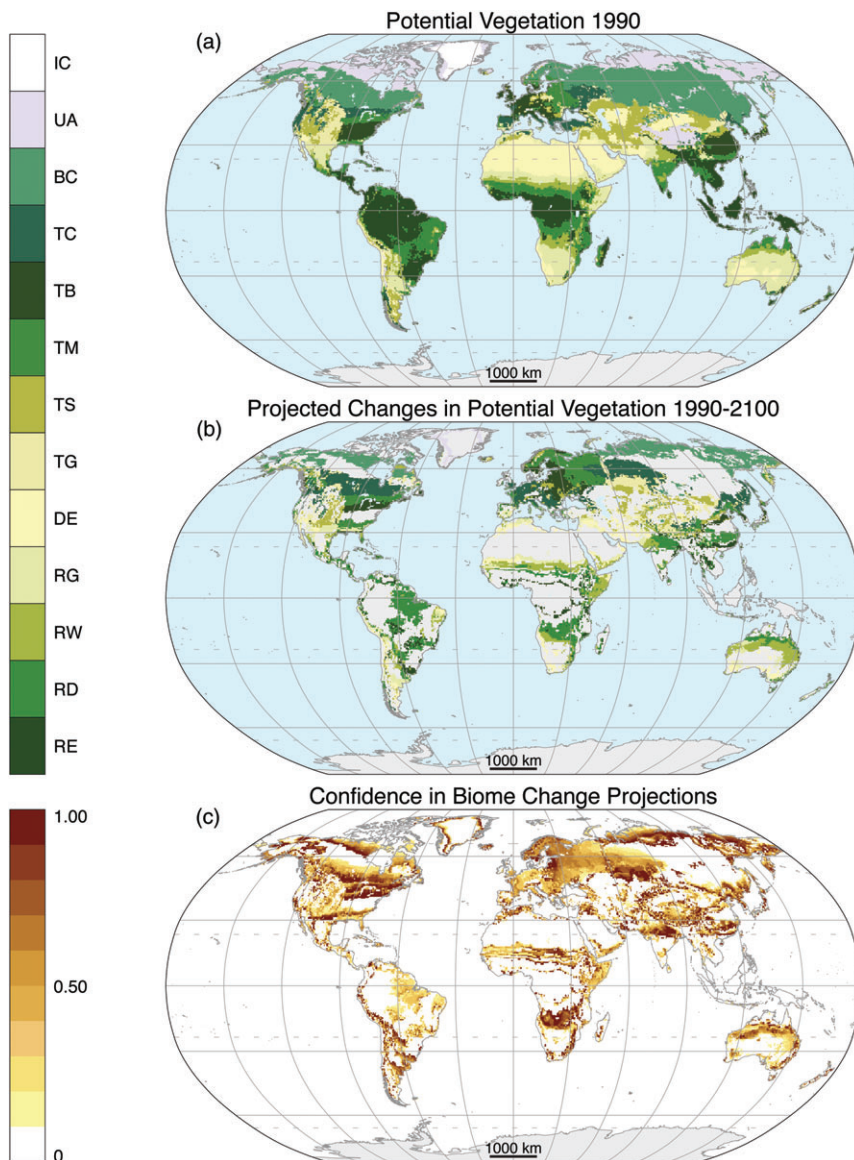


**Figure 3** Vegetation projections. (a) MC1-modelled potential vegetation under observed 1961–90 climate. (b) MC1-modelled potential vegetation under projected 2071–2100 climate where any of nine general circulation model–emissions scenario combinations projects a change. Biomes, in (a) and (b), from poles to equator: ice (IC), tundra and alpine (UA), boreal conifer forest (BC), temperate conifer forest (TC), temperate broadleaf forest (TB), temperate mixed forest (TM), temperate shrubland (TS), temperate grassland (TG), desert (DE), tropical grassland (RG), tropical woodland (RW), tropical deciduous broadleaf forest (RD), tropical evergreen broadleaf forest (RE). (c) Confidence of biome projections calculated from fraction of general circulation model–emissions scenario combinations that project the same type of biome change.

vulnerable to biome changes (Table 2). Vegetation projections indicate low to very low vulnerability of ecosystems to biome change on up to two-thirds of global land. Patterns of vulnerability derived from observed climate alone (Fig. 4a) differ from the patterns derived from all nine vegetation projections combined (Fig. 4b). The overlap of observed climate and the nine vegetation projections (Fig. 4c) identifies areas that both indicators identify as highly to very highly vulnerable: the Andes, the Baltic coast, boreal Canada and Russia, the Himalayas, the Iberian Peninsula, the Laurentian Great Lakes, northern Brazil and southern Africa.

Vegetation projections for individual emissions scenarios show areas of vulnerability under A1B and A2 that are, respectively, one-third and one-half greater than under B1 (Table 2, Appendix S4). The overlap of observed climate and vegetation projections for individual emissions scenarios show areas of vulnerability under A1B and A2 that are, respectively, one-

quarter and one-half greater than under B1 (Table 2, Appendix S5). Among the emissions scenarios, the general patterns of vulnerability remain consistent – it is the size of highly vulnerable patches that expands with increasing emissions.

Temperate mixed and boreal conifer forests show the highest vulnerability as a fraction of biome area, while tundra and alpine and boreal conifer forest biomes are most vulnerable in total land area (Fig. 5, Table 2). Deserts show the lowest vulnerability as a fraction of biome area for most cases, while all cases show tropical evergreen broadleaf forest as least vulnerable in total land area.

Approximately 3 billion people, or half of the world’s population, live in areas of high to very high vulnerability under observed climate only (Table 2). Approximately 800 million to 1.3 billion people, or one-eighth to one-fifth of the world’s population, live in areas of high to very high vulnerability under the other cases.



**Table 2** Global areas of vulnerability to biome change, population of highly vulnerable areas and most and least vulnerable biomes.

Case	Vulnerable areas					Population of very highly and highly vulnerable areas		Most vulnerable as fraction of biome area		Most vulnerable in total land area		Least vulnerable as fraction of biome area		Least vulnerable in total land area		
	Very high	High	Medium	Low	Very low	(10 <sup>9</sup> people)	Biome	Biome	Area (10 <sup>6</sup> km <sup>2</sup> )	Biome	Area (10 <sup>6</sup> km <sup>2</sup> )	Biome	Area (10 <sup>6</sup> km <sup>2</sup> )	Biome	Area (10 <sup>6</sup> km <sup>2</sup> )	
	(% of global land area)															(% of area)
OC	12	36	49	2	1	3.3	BC	BC	65	BC	13	RW	RW	7	RE	1
PV9	8	4	33	5	50	0.9	TM	UA	35	UA	3	DE	DE	88	RE	17
PVA2	16	—	30	—	53	1.2	TM	UA	47	UA	5	DE	DE	86	RE	16
PVA1B	13	—	32	—	55	1.0	TM	UA	41	UA	4	DE	DE	88	RE	16
PVB1	10	—	25	—	64	0.8	TM	UA	33	UA	3	DE	DE	90	RE	18
OC-PV9	1	11	62	25	1	1.0	TM	UA	33	UA	3	DE	DE	38	RE	8
OC-PVA2	1	17	54	27	1	1.3	TM	UA	48	UA	5	DE	DE	39	RE	8
OC-PVA1B	1	15	56	27	1	1.3	TM	UA	43	UA	4	DE	DE	40	RE	8
OC-PVB1	1	11	55	32	1	1.0	TM	UA	35	UA	3	TB	TB	41	RE	9

Results are shown for nine alternative cases: observed 20th-century climate change (OC), projected 21st-century vegetation under unanimous agreement of three IPCC emissions scenarios and three GCMs (PV9), projected 21st-century vegetation under three IPCC emissions scenarios (PVA2, PVA1B, PVB1) and the overlap of observed climate change and projected vegetation (OC-PV9, OC-PVA2, OC-PVA1B, OC-PVB1). Listed biomes include boreal conifer forest (BC), desert (DE), temperate broadleaf forest (TM), temperate mixed forest (TB), tropical evergreen broadleaf forest (RE), tropical woodland (RW) and tundra and alpine (UA).

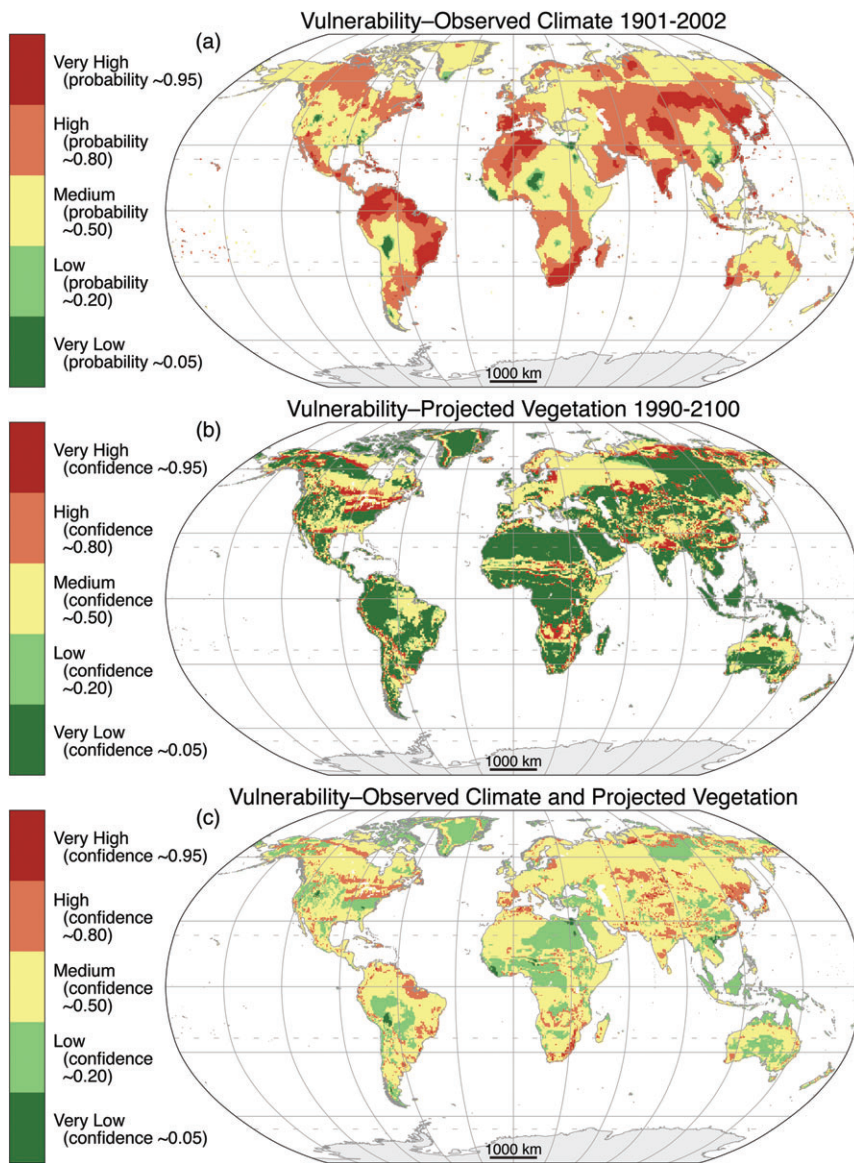


**Figure 4** Vulnerability to biome change based on (a) 20th-century observed climate, (b) 21st-century vegetation projections under nine general circulation model–emissions scenario combinations, and (c) overlap of (a) and (b). Vulnerability classes use IPCC (2007a) confidence class names and levels.

## DISCUSSION

### Global vulnerability

All cases of observed climate, projected vegetation and their overlap show high to very high vulnerability of a substantial fraction of global land. Even under the lowest emissions scenario, the indicators identify extensive areas of potentially substantial ecological change.

Observed climate changes signal high vulnerability for almost half of the global land area. Vegetation projections suggest potential latitudinal biome shifts of up to 400 km, consistent with projections of individual species range shifts (Morin & Thuiller, 2009). Confidence in vegetation projections shows latitudinal gradients along ecotones and fragmented patterns in core areas, as previously theorized (Neilson, 1993). Confidence is higher at the trailing edges of latitudinal biomes than at

leading edges, analogous to the upslope leaning of species distribution curves that shift along an elevation gradient (Kelly & Goulden, 2008).

Temperate mixed forest shows high vulnerability as a fraction of biome area due to projected loss of coniferous species and potential conversion to temperate broadleaf forest. The tundra and alpine biome shows the greatest total area of high to very high vulnerability due to elevated rates of both observed and projected warming. Tropical evergreen broadleaf forest shows low vulnerability. The resilience of rain forests derives from high temperature tolerances and mitigation of water stress by increases in equatorial precipitation (Malhi *et al.*, 2008) as well as the wide latitudinal extent of woody plant species (Weiser *et al.*, 2007).

Spatial patterns of change and vulnerability agree substantially with previous analyses at coarser scales. The patterns of observed climate change agree with analyses (Vose *et al.*, 2005;

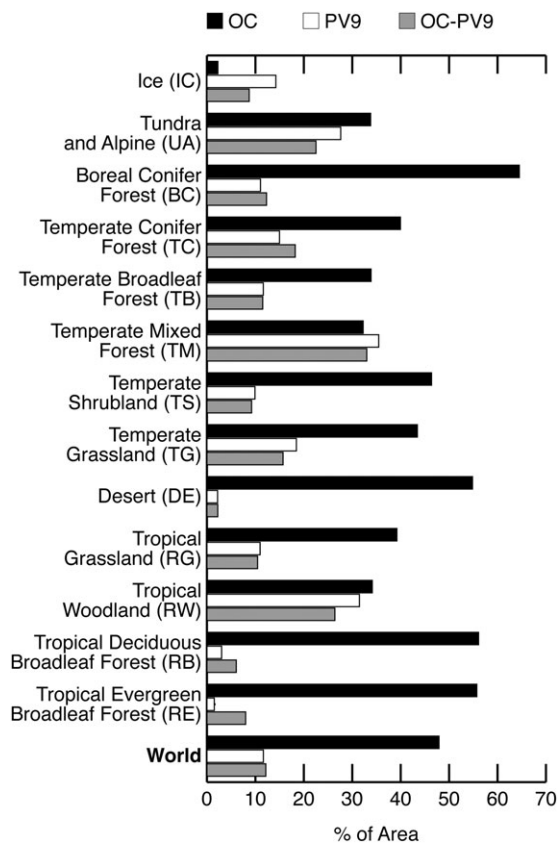


**Figure 5** Fraction of biome area in areas of high to very high vulnerability under observed climate (OC, black), vegetation projections under nine general circulation model–emissions scenario combinations (PV9, white), overlap of observed climate and vegetation projections under nine general circulation model–emissions scenario combinations (OC–PV9, grey).

Dang *et al.*, 2007; Trenberth *et al.*, 2007) of climate data (Jones *et al.*, 2001; Smith & Reynolds, 2005) at a spatial resolution coarser than the data here by an order of magnitude. MC1 vegetation projections are consistent with results from the Community Land Model (Alo & Wang, 2008), the HadCM3LC coupled GCM–DGVM (Jones *et al.*, 2009), the Lund–Potsdam–Jena (LPJ) DGVM (Scholze *et al.*, 2006) and four other DGVMs (Sitch *et al.*, 2008), run at spatial resolutions coarser than the data here by factors of 3, 5, 5.6 and 7.5, respectively. The DGVMs project a shift of boreal forest into tundra at high latitudes and some forest loss in Amazonia. Both MC1 and LPJ project forest changes in the southeastern USA and East Asia, although they disagree on changes in India. MC1 results are also consistent with non-dynamic climate and vegetation modelling (Lee & Jetz, 2008). MC1 and LPJ produce consistent wildfire results, projecting increases in the Amazon, Australia, southern Africa and the western USA. Our vulnerability results agree with a vulnerability analysis based on potential novel climates (Williams *et al.*, 2007) in the African Sahel, the Andes, the northern Amazon and other areas, but do not agree in some equatorial and temperate areas because the novel climate index more heavily weights areas of low inter-annual variability.

We find that a large part of the world’s population lives in areas of potential biome changes. This includes up to one-fifth of the world’s population and up to one-quarter of the population in Asia and North and South America. Biome changes may alter the provision of ecosystem services (Schröter *et al.*, 2005), possibly affecting the livelihoods of many of these people. For example, certain biome changes could change the density of tree species used for firewood or timber or the density of grass species preferred for grazing, alter the water retention capacity in watersheds providing drinking water for human use, or change patterns of fire and other disturbances integral to ecosystem function.

### Limitations of interpretation

To produce results at a spatial scale useful for assessing potential impacts of climate change on vegetation, we applied empirical statistical downscaling to the coarse GCM output. Our method adjusts GCM output by observed 50-km climate patterns so that downscaled data exhibit the climate differences of the GCM projections while retaining the relative spatial patterns of observed climate. The continental and global averages of projected temperature and precipitation changes of the downscaled results (Table 1) are close to the corresponding averages of the coarse GCM ensembles (IPCC, 2007a), suggesting that our downscaled climate projections retain broad agreement with the GCM output. IPCC has confirmed the validity of empirical statistical downscaling of climate scenarios for impacts analyses (Christensen *et al.*, 2007). Drawbacks include an assumption of relative stability of cross-scale climate relationships and increased uncertainty in spatial changes finer than the coarse resolution of the original GCM output. Because the spatial resolution of the original GCM output is approximately 250 km (north–south) by 375 km (east–west), conclusions about results at finer scales are still uncertain.

Use of the biome as a unit of analysis may understate vulnerability because the broad definition of a biome allows for changes in species composition without conversion to a different biome. Although MC1 DGVM projections of potential vegetation change will increase at more detailed levels of a classification hierarchy (Neilson, 1993), the 77% agreement of modelled with observed forest cover suggests the use of a level no lower than the biome for this analysis. Biome change provides a useful indicator of vulnerability because climate changes severe enough to convert the biome of an area are likely to signal more serious impacts at lower levels. The analyses do not explicitly examine reductions of tree density that may occur in episodes of forest dieback without changing the biome of an area (Scholze *et al.*, 2006; Jones *et al.*, 2009). This may further understate vulnerability.

The kappa value for MC1 is in the range considered ‘fair’ (Monserud & Leemans, 1992), suggesting caution in the use of DGVM output. For this reason, we have examined one case (labelled PV9 in Table 2) that uses a stringent and restrictive criterion of unanimous agreement for the very high vulnerability class. In addition, we examine four cases (OC–PV9,

OC-PVA2, OC-PVA1B, OC-PVB1) that overlap vulnerability results from observed climate and vulnerability results of vegetation projections to find where observations and projections might show similar patterns.

DGVMs delineate potential, not realized, vegetation distributions. Survival and dispersal capabilities of species, human barriers to dispersal, interspecific competition, evolutionary adaptation, changing pests and pathogens and other factors will lead to biome changes occurring at varying rates. In some cases, rates of climate change may exceed the dispersal abilities of individual species. Conditions projected for AD 2100 may reflect committed changes, but long time-scales of atmospheric equilibrium and ecological processes create a double transient situation. Global terrestrial vegetation may continue to change long after climate stabilization (Jones *et al.*, 2009).

Direct human modification of land cover, which this analysis does not explicitly include, could interact with climate change (Lee & Jetz, 2008). Even though our analysis identifies tropical rain forests as less vulnerable to climate change, continued deforestation for timber harvesting and agricultural expansion would nullify that advantage.

The population analysis approximates the number of people living in areas classified as most and least vulnerable to vegetation shifts. Although more complex analyses could quantify negative and positive impacts on ecosystem services and account for differences due to the extent of agricultural and urban areas, the estimates indicate the orders of magnitude of the human population of the different vulnerability classes.

### Adaptation of natural resource management

Adaptation is an adjustment in natural or human systems in response to actual or expected climatic stimuli or their effects, to moderate harm or exploit beneficial opportunities (IPCC, 2007b). Analyses of vulnerability and prioritization of locations, ecosystems or species can guide the planning of adaptation measures (Hannah *et al.*, 2002). The mismatch between the patterns of vulnerability identified here and the geographic priorities of global organizations (Brooks *et al.*, 2006) suggests the need to adapt current management plans to climate change. We have sought to develop a vulnerability analysis framework with clearly defined classes easily interpreted by natural resource managers. Furthermore, we have sought to provide data to help prioritize existing and future national and regional forests, parks, reserves and other natural areas for adaptation measures.

To identify geographic priorities under climate change, managers can broadly consider three options: areas of high, medium or low vulnerability of ecosystems to biome change. For the acquisition of new areas, it may be prudent to prioritize areas of potentially greater resilience, known as refugia, and to avoid areas of higher vulnerability, all other factors being equal. Conversely, for the management of existing areas, it may be necessary to prioritize places of higher vulnerability for adaptation measures because those locations may require more intensive management, such as prescribed burning to avoid catastrophic wildfire and invasive species removal, because of potentially

greater disturbances and species turnover. Areas of unique ecological or cultural value may continue to merit high priority. The eventual configuration of new and existing natural resource areas may also reveal appropriate areas for the establishment of corridors to facilitate species dispersal and migration. Although the coarse scale of our results only provides information appropriate for global and regional planning, application of our method to data at finer spatial scales (Ashcroft *et al.*, 2009), subject to accuracy limits of downscaling, could make climate change planning possible for local areas. In addition to adaptation measures, substantial reductions in greenhouse gas emissions could enable the world to avoid the most serious consequences of climate change, which include global vegetation shifts and potential impacts on human well-being.

### ACKNOWLEDGEMENTS

For the IPCC climate projection data we acknowledge the GCM modelling groups, the Program for Climate Model Diagnosis and Intercomparison, and the World Climate Research Programme for the WCRP CMIP3 multi-model data set, supported by the US Department of Energy. We gratefully acknowledge comments from C. D. Allen, G. C. Daily, B. Griffith, L. Hannah, S. H. Schneider, J. M. Scott, C. J. Tucker and J. A. Wiens, work on MC1 by D. Bachelet and J. R. Wells, and funding from the Nature Conservancy and the USDA Forest Service.

### REFERENCES

- Alo, C.A. & Wang, G. (2008) Potential future changes of the terrestrial ecosystem based on climate projections by eight general circulation models. *Journal of Geophysical Research*, **113**, G01004, doi:10.1029/2007JG000528.
- Ashcroft, M.B., Chisholm, L.A. & French, K.O. (2009) Climate change at the landscape scale: Predicting fine-grained spatial heterogeneity in warming and potential refugia for vegetation. *Global Change Biology*, **15**, 656–667.
- Bartholomé, E. & Belward, A.S. (2005) GLC2000: A new approach to global land cover mapping from Earth observation data. *International Journal of Remote Sensing*, **26**, 1959–1977.
- Beckage, B., Osborne, B., Gavin, D.G., Pucko, C., Siccama, T. & Perkins, T. (2008) A rapid upward shift of a forest ecotone during 40 years of warming in the Green Mountains of Vermont. *Proceedings of the National Academy of Sciences of the USA*, **105**, 4197–4202.
- Brooks, T.M., Mittermeier, R.A., Fonseca, G.A.B., Gerlach, J., Hoffmann, M., Lamoreux, J.F., Mittermeier, C.G., Pilgrim, J.D. & Rodrigues, A.S.L. (2006) Global biodiversity conservation priorities. *Science*, **313**, 58–61.
- Christensen, J.H., Hewitson, B., Busuioc, A., Chen, A., Gao, X., Held, I., Jones, R., Kolli, R.K., Kwon, W.T., Laprise, R., Magaña Rueda, V., Mearns, L., Menéndez, C.G., Räisänen, J., Rinke, A., Sarr, A. & Whetton, P. (2007) Regional climate projections. *Climate change 2007: The physical science basis* (Intergovernmental Panel on Climate Change), pp. 847–940. Cambridge University Press, Cambridge.

- Cohen, J. (1960) A coefficient of agreement for nominal scales. *Educational and Psychological Measurement*, **20**, 37–46.
- Daly, C., Bachelet, D., Lenihan, J.M., Neilson, R.P., Parton, W. & Ojima, D. (2000) Dynamic simulation of tree–grass interactions for global change studies. *Ecological Applications*, **10**, 449–469.
- Dang, H., Gillett, N.P., Weaver, A.J. & Zwiers, F.W. (2007) Climate change detection over different land surface vegetation classes. *International Journal of Climatology*, **27**, 211–220.
- Davis, M.B. & Shaw, R.G. (2001) Range shifts and adaptive responses to Quaternary climate change. *Science*, **292**, 673–679.
- FAO (2001) *Global Forest Resources Assessment 2000*. Food and Agriculture Organization, Rome.
- Gonzalez, P. (2001) Desertification and a shift of forest species in the West African Sahel. *Climate Research*, **17**, 217–228.
- Gordon, H.B., Rotstayn, L.D., McGregor, J.L., Dix, M.R., Kowalczyk, E.A., O’Farrell, S.P., Waterman, L.J., Hirst, A.C., Wilson, S.G., Collier, M.A., Watterson, I.G. & Elliott, T.I. (2002) *The CSIRO Mk3 climate system model*. Atmospheric Research Technical Paper No. 60. Commonwealth Scientific, Industrial, and Research Organisation, Victoria.
- Hannah, L., Midgley, G.F. & Millar, D. (2002) Climate change-integrated conservation strategies. *Global Ecology and Biogeography*, **11**, 485–495.
- Hasumi, H. & Emori, S. (2004) *K-1 Coupled Model (MIROC) description*. K-1 Technical Report No. 1. Center for Climate System Research, University of Tokyo, Tokyo.
- IPCC (2007a) *Climate Change 2007: The physical science basis*. Cambridge University Press, Cambridge.
- IPCC (2007b) *Climate change 2007: Impacts, adaptation, and vulnerability*. Cambridge University Press, Cambridge.
- Jackson, S.T. & Overpeck, J.T. (2000) Responses of plant populations and communities to environmental changes of the late Quaternary. *Paleobiology*, **26**, 194–220.
- Johns, T.C., Gregory, J.M., Ingram, W.J., Johnson, C.E., Jones, A., Lowe, J.A., Mitchell, J.F.B., Roberts, D.L., Sexton, D.M.H., Stevenson, D.S., Tett, S.F.B. & Woodage, M.J. (2003) Anthropogenic climate change for 1860 to 2100 simulated with the HadCM3 model under updated emissions scenarios. *Climate Dynamics*, **20**, 583–612.
- Jones, C., Lowe, J., Liddicoat, S. & Betts, R. (2009) Committed terrestrial ecosystem changes due to climate change. *Nature Geoscience*, **2**, 484–487.
- Jones, P.D., Osborn, T.J., Briffa, K.R., Folland, C.K., Horton, E.B., Alexander, L.V., Parker, D.E. & Rayner, N.A. (2001) Adjusting for sampling density in grid box land and ocean surface temperature time series. *Journal of Geophysical Research*, **106**, 3371–3380.
- Kelly, A.E. & Goulden, M.L. (2008) Rapid shifts in plant distribution with recent climate change. *Proceedings of the National Academy of Sciences of the USA*, **105**, 11823–11826.
- Kuchler, A.W. (1964) *Potential natural vegetation of the conterminous United States*. American Geographical Society Special Publication No. 36. American Geographical Society, New York.
- Kullman, L. & Öberg, L. (2009) Post-Little Ice Age tree line rise and climate warming in the Swedish Scandes: A landscape ecological perspective. *Journal of Ecology*, **97**, 415–429.
- Lee, T.M. & Jetz, W. (2008) Future battlegrounds for conservation under global change. *Proceedings of the Royal Society B: Biological Sciences*, **275**, 1261–1270.
- Lenihan, J.M., Bachelet, D., Neilson, R.P. & Drapek, R. (2008) Response of vegetation distribution, ecosystem productivity, and fire to climate change scenarios for California. *Climatic Change*, **87**, 215–230.
- Malhi, Y., Roberts, J.T., Betts, R.A., Killeen, T.J., Li, W. & Nobre, C.A. (2008) Climate change, deforestation, and the fate of the Amazon. *Science*, **319**, 169–172.
- Mitchell, T.D. & Jones, P.D. (2005) An improved method of constructing a database of monthly climate observations and associated high-resolution grids. *International Journal of Climatology*, **25**, 693–712.
- Monserud, R.A. & Leemans, R. (1992) Comparing global vegetation maps with the Kappa statistic. *Ecological Modelling*, **62**, 275–293.
- Morin, X. & Thuiller, W. (2009) Comparing niche- and process-based models to reduce prediction uncertainty in species range shifts under climate change. *Ecology*, **90**, 1301–1313.
- Mouillot, F. & Field, C.B. (2005) Fire history and the global carbon budget: A 1° × 1° fire history reconstruction for the 20<sup>th</sup> century. *Global Change Biology*, **11**, 398–420.
- Neilson, R.P. (1993) Transient ecotone response to climatic change: Some conceptual and modelling approaches. *Ecological Applications*, **3**, 385–395.
- Norby, R.J., DeLucia, E.H., Gielen, B., Calfapietra, C., Giardina, C.P., King, J.S., Ledford, J., McCarthy, H.R., Moore, D.J.P., Ceulemans, R., De Angelis, P., Finzi, A.C., Karnosky, D.F., Kubiske, M.E., Lukac, M., Pregitzer, K.S., Scarascia-Mugnozza, G.E., Schlesinger, W.H. & Oren, R. (2005) Forest response to elevated CO<sub>2</sub> is conserved across a broad range of productivity. *Proceedings of the National Academy of Sciences of the USA*, **102**, 18052–18056.
- Parmesan, C. & Yohe, G. (2003) A globally coherent fingerprint of climate change impacts across natural systems. *Nature*, **421**, 37–42.
- Peñuelas, J. & Boada, M. (2003) A global change-induced biome shift in the Montseny mountains (NE Spain). *Global Change Biology*, **9**, 131–140.
- Raupach, M.R., Marland, G., Ciais, P., Le Quéré, C., Canadell, J.G., Klepper, G. & Field, C.B. (2007) Global and regional drivers of accelerating CO<sub>2</sub> emissions. *Proceedings of the National Academy of Sciences of the USA*, **104**, 10288–10293.
- Rosenzweig, C., Casassa, G., Karoly, D.J., Imeson, A., Liu, C., Menzel, A., Rawlins, S., Root, T.L., Seguin, B. & Tryjanowski, P. (2007) Assessment of observed changes and responses in natural and managed systems. *Climate Change 2007: Impacts, adaptation and vulnerability* (Intergovernmental Panel On Climate Change), pp. 79–131. Cambridge University Press, Cambridge.
- Rosenzweig, C., Karoly, D., Vicarelli, M., Neofotis, P., Wu, Q., Casassa, G., Menzel, A., Root, T.L., Estrella, N., Seguin, B.,

- Tryjanowski, P., Liu, C., Rawlins, S. & Imeson, A. (2008) Attributing physical and biological impacts to anthropogenic climate change. *Nature*, **453**, 353–357.
- Schneider, S.H., Semenov, S., Patwardhan, A., Burton, I., Magadza, C.H.D., Oppenheimer, M., Pittock, A.B., Rahman, A., Smith, J.B., Suarez, A. & Yamin, F. (2007) Assessing key vulnerabilities and the risk from climate change. *Climate Change 2007: Impacts, adaptation and vulnerability* (Intergovernmental Panel on Climate Change), pp. 779–810. Cambridge University Press, Cambridge.
- Scholze, M., Knorr, W., Arnell, N.W. & Prentice, I.C. (2006) A climate-change risk analysis for world ecosystems. *Proceedings of the National Academy of Sciences of the USA*, **103**, 13116–13120.
- Schröter, D., Cramer, W., Leemans, R. *et al.* (2005) Ecosystem service supply and vulnerability to global change in Europe. *Science*, **310**, 1333–1337.
- Sitch, S., Huntingford, C., Gedney, N., Levy, P.E., Lomas, M., Piao, S.L., Betts, R., Ciais, P., Cox, P., Friedlingstein, P., Jones, C.D., Prentice, I.C. & Woodward, F.I. (2008) Evaluation of the terrestrial carbon cycle, future plant geography and climate-carbon cycle feedbacks using five dynamic global vegetation models (DGVMs). *Global Change Biology*, **14**, 2015–2039.
- Smith, T.M. & Reynolds, R.W. (2005) A global merged land and sea surface temperature reconstruction based on historical observations (1880–1997). *Journal of Climate*, **18**, 2021–2036.
- Trenberth, K.E., Jones, P.D., Ambenje, P., Bojariu, R., Easterling, D., Klein Tank, A., Parker, D., Rahimzadeh, F., Renwick, J.A., Rusticucci, M., Soden, B. & Zhai, P. (2007) Observations: surface and atmospheric climate change. *Climate Change 2007: The physical science basis* (Intergovernmental Panel on Climate Change), pp. 235–336. Cambridge University Press, Cambridge.
- VEMAP Members (1995) Vegetation/ecosystem modeling and analysis project: Comparing biogeography and biogeochemistry models in a continental-scale study of terrestrial ecosystem responses to climate change and CO<sub>2</sub> doubling. *Global Biogeochemical Cycles*, **9**, 407–437.
- Vose, R.S., Easterling, D.R. & Gleason, B. (2005) Maximum and minimum temperature trends for the globe: An update through 2004. *Geophysical Research Letters*, **32**, L23822, doi:10.1029/2005GL024379.
- Weiser, M.D., Enquist, B.J., Boyle, B., Killeen, T.J., Jørgensen, P.M., Fonseca, G., Jennings, M.D., Kerkhoff, A.J., Lacher, T.E., Monteagudo, A., Núñez Vargas, M.P., Phillips, O.L., Swenson, N.G. & Vásquez Martínez, R. (2007) Latitudinal patterns of range size and species richness of New World woody plants. *Global Ecology and Biogeography*, **16**, 679–688.
- Williams, J.W., Jackson, S.T. & Kutzbach, J.E. (2007) Projected distributions of novel and disappearing climates by 2100 AD. *Proceedings of the National Academy of Sciences of the USA*, **104**, 5738–5742.
- Woodward, F.I., Lomas, M.R. & Kelly, C.K. (2004) Global climate and the distribution of plant biomes. *Philosophical Transactions of the Royal Society B: Biological Sciences*, **359**, 1465–1476.

## SUPPORTING INFORMATION

Additional Supporting Information can be found in the on-line version of this article:

**Appendix S1** Observed biome shifts

**Appendix S2** Ranges of  $P_{\text{climate}}$  and  $c_{\text{projection}}$  that define vulnerability classes.

**Appendix S3** Areas of projected biome change by biome.

**Appendix S4** Vulnerability from analyses of vegetation projections by emissions scenario.

**Appendix S5** Vulnerability from overlap of observed climate and projected vegetation by emissions scenario.

As a service to our authors and readers, this journal provides supporting information supplied by the authors. Such materials are peer-reviewed and may be re-organized for online delivery, but are not copy-edited or typeset. Technical support issues arising from supporting information (other than missing files) should be addressed to the authors.

## BIOSKETCH

**Patrick Gonzalez** is a Visiting Scholar in the Center for Forestry, University of California, Berkeley. He conducts applied research on impacts of climate change, adaptation of natural resource management, and forest carbon, and has served as a lead author for the Intergovernmental Panel on Climate Change.

Editor: Brad Murray